Production of sodium-based zeolites and a potassium-containing leach liquor by alkaline leaching of South African coal fines ash

A.C. Collins[1], C.A. Strydom[2], R.H. Matjie[3], J.R. Bunt[3], and J.C. van Dyk[1,4]

Affiliation:
[1] Chemical Resource Beneficiation, North-West University, Potchefstroom Campus, Potchefstroom.
[2] Centre of Excellence in Carbon-based Fuels, School of Physical and Chemical Sciences, North-West University, Potchefstroom Campus, Potchefstroom.
[3] Centre of Excellence in Carbon-based Fuels, School of Chemical and Mineral Engineering, North-West University, Potchefstroom Campus, Potchefstroom.
[4] African Carbon Energy, South Africa.

Correspondence to:
R.H. Matjie

Email:
matjie4@gmail.com

Synopsis

South African coal discards derived from feed coal for thermoprocesses pose human health and environmental problems and incur high disposal costs. These issues need to be resolved. Coal fines and a coal fines/ K_2CO_3 blend were combusted at 700°C in a laboratory rotary kiln to produce ashes containing metakaolinite ($Al_2O_3.2SiO_2$) and illite/muscovite/orthoclase amorphous materials. The blend ash and coal fines ash, containing 18% K_2O and <1% K_2O respectively, were leached with water and with 1 M and 8 M NaOH at 80°C for 4 hours using a solid to liquid ratio of 1:5. The 8 M NaOH leach yielded 17% sodalite ($Na_8Si_6Al_6O_{24}(OH)_2$) formation through SiO_3^{2-}, $Al(OH)_4^{-}$, and Na^+ precipitation in the leached ashes. The 1 M NaOH leach yielded no sodalite. X-ray fluorescence analysis of the original ashes and leached ashes showed low Al and Si dissolution efficiencies due to the sodalite formation. Sequential NaOH leaching resulted in the highest potassium dissolution efficiency of 89% for the ashes of fines/K_2CO_3 blend and 59% for the fines. It may be possible to increase the ash-derived zeolite concentration by using even higher NaOH concentrations (12–20 M NaOH) during leaching. Sodalite derived from coal ash could possibly be utilized for water purification in industrial applications, or as molecule separators. The potassium-containing liquid could be used in fertilizer manufacture.

Keywords

low-temperature combustion coal ash, alkaline leaching, sodalite, potassium leach liquor.

Introduction

Commercial power stations in many countries around the world utilize pulverized run-of-mine (ROM) feed coal (<75 μm) to produce electricity (Bukhari *et al.*, 2015). Due to population growth and industrialization the demand for power is increasing (Izquierdo and Querol, 2012). During coal mining and feed preparation in South Africa, approximately 60 Mt of coal fines (byproduct) are generated and discarded per annum (Reddick, von Blottnitz, and Kothuis, 2007; Bunt *et al.*, 2015). These coal discards have similar chemical and mineralogical properties to South African gasification and combustion ROM feed coals; however, they are characterized by a higher mineral matter (48% versus 29–32%) and higher-vitrinite (26% *versus* 24%) content (Matjie *et al.*, 2015; Bunt *et al.*, 2015; Rautenbach *et al.*, 2019; 2020). Globally, colliery and thermochemical plant activities generate 30 Gt of coal fine discards annually. High costs are associated with the treatment and disposal of these wastes. They contribute significantly to dust generation and acid mine drainage, and are prone to spontaneous combustion (Reddick, von Blottnitz, and Kothuis, 2007). These negative environmental impacts need to be addressed.

Combustion of pulverized fuel (PF) in coal-fired power plants generates a number of byproducts (Nayak and Panda, 2010). Coal ash, comprising coal fly ash (CFA) and coal bottom ash (CBA) (the main constituent) produced during coal combustion, is one of these byproducts (Bukhari *et al.*, 2015). The scope for utilizing these byproducts in other industrial applications is limited (Nayak and Panda, 2010), and the bulk of the ash is discarded into landfills (Murayama, Yamamoto, and Shibata, 2002). The CBA and CFA, which contain zero or trace amounts of mullite ($Al_6O_{13}Si_2$) and anorthite ($CaAl_2Si_2O_8$), have the potential to serve as starting materials in the production of gibbsite ($Al(OH)_3$), due to their high aluminium content (Su *et al.*, 2011; Yang, Zheng, and Zhang, 2014).

The recovery of aluminium from CBA and CFA containing higher proportions of mullite and anorthite has been the focus of many investigations (King *et al.*, 2018; Li *et al.*, 2014; Bunt *et al.*, 1998; Yang, Zheng, and Zhang, 2014). Recovery methods include acid leaching of CBA and CFA (Bunt *et al.*, 1998; Sangita, Nayak, and Panda, 2017), alkaline leaching of CBA and CFA (Li *et al.*, 2014; Su *et al.*, 2011), ammonium sulphate ($NH_4)_2(SO_4)$) roasting of CFA (van der Merwe *et al.*, 2017), and in some investigations a

Production of sodium-based zeolites and a potassium-containing leach liqour by alkaline leaching

combination of these methods. Investigations of alkaline leaching of ash or solid waste materials have shown that the concentration and type of alkaline lixiviant influence the dissolution of the inorganic components. Alumina (Al_2O_3), silica (SiO_2), and aluminium silicate precursors, which are the starting point for a variety of compounds, are mostly obtained by mixing of the CBA/CFA with an alkaline solution (Comrie and Kriven, 2004). Adrian and McCulloch (1966) found that 90% recovery of Al from South African CBA/CFA with low or zero mullite content could be achieved at high leaching temperatures and sodium hydroxide (NaOH) concentrations. However, even with high dissolution the process was not considered economically viable.

Yang, Zheng, and Zhang (2014) reported that an alumina extraction efficiency of 92% was attained by NaOH leaching of a desilicated product containing zero mullite/anorthite from Chinese CFA with a molar ratio of CaO to SiO_2 of 1:1 at elevated temperatures and pressures. Furthermore, the formation of $NaCaHSiO_4$ captures the silica and inhibits zeolite formation. Su *et al.* (2011) stated that a two-step NaOH leach of CFA achieved 89% aluminium dissolution efficiency and that the formation of sodalite ($Na_8Si_6Al_6O_{24}(OH)_2)$) occurred during the first step. Aside from being used to recover inorganic elements, this method has also been used for synthesizing zeolite crystals (Fukasawa *et al.*, 2017). The alkaline solution dissolves aluminium silicates and silica from heated CFA to form silicate and aluminate ions during the NaOH leaching step (Jiang *et al.*, 2015). These ions precipitate and subsequently crystallize on the surface of the CFA particles. Leaching conditions such as the reaction temperature, lixiviant concentration, and leaching time influence the dissolution efficiencies of aluminium and silicon, as well as zeolite formation. In this investigation, the lixiviants referred to are liquid media used in the hydrometallurgical processes to selectively dissolve high-value inorganic elements associated with minerals contained in either CFA/CBA or ores. Fukasawa *et al.* (2017) found that pulverization of the ash prior to the hydrothermal treatment, increased the surface area, which in turn increased the dissolution of alumina and silica species; if these species do not form part of the inert mullite and feldspars, a high proportion of zeolite is formed.

South African commercial power stations combust PF at elevated temperature (approximately 1600°C), producing CBA and CFA (Rautenbach *et al.*, 2021; van Alphen, 2005). These ashes comprise mainly mullite and quartz (SiO_2) with small amounts of anorthite and cristobalite (SiO_2) (Rautenbach *et al.*, 2021), which are insoluble in NaOH solution at a leaching temperature of 80°C. These conditions were not used in this study as they are not suitable to produce low-temperature combustion ashes (containing soluble Al, Si, K, and Ti species) from coal fines and coal fines and K_2CO_3 blends for NaOH leaching.

The aim of this novel investigation was to use alkaline solutions in an attempt to dissolve Al, K, Si, and Ti from illite ($(K, H_3O)(Al,Mg,Fe)_2(Si,Al)$), orthoclase ($KAlSi_3O_8$), muscovite ($KAl_2(AlSi_3O_{10}(FOH)_2)$), and metakaolinite ($Al_2O_3.2SiO_2$) amorphous materials contained in the low-temperature combustion ashes. These ashes, with unique chemical and mineralogical properties, were prepared in a laboratory rotary kiln by combusting discarded coal fines (designated SA1) and a blend of ROM feed coal and K_2CO_3 (designated SA2 blend) at 700°C. The influence of K_2CO_3 addition on the dissolution efficiency of Al, K, Si, and Ti from illite, muscovite, and orthoclase amorphous phases, metakaolinite, and K species in these low-temperature combustion ashes was investigated. Additionally, the catalytic effect of the heated K_2CO_3 on zeolite formation from these ashes was investigated.

Neither the effect of K_2CO_3 addition nor NaOH concentration on the dissolution efficiency of high-value inorganic elements and zeolite formation from low-temperature combustion ashes have been investigated previously. The potassium species and OH^- in this ash could also promote precipitation of the zeolite gel precursor and the subsequent crystallization of sodalite in the leached ash.

The original ash and leached ash samples were submitted for X-ray fluorescence (XRF) and the X-ray diffraction (XRD) analyses. The XRF results were used in the calculations of the dissolution efficiencies of the selected inorganic elements (Al, K, Si and Ti) after leaching of the ash samples with deionized water and sodium hydroxide solutions.

The sodium-based zeolite (sodalite) derived from low-temperature combustion ash has potential for industrial applications such as water and gas purification. Furthermore, the leach liquor containing potassium species could possibly be used as liquid fertilizer.

Materials and methods

Coals sampling, preparation, reagents, and coal composition

The coal fines discards (SA1 and SA2) were derived from two ROM medium-volatile bituminous South African coals from the Highveld Coalfield. The samples were air-dried for 2 days to reduce excess moisture not associated with the coal structure. After drying, each sample was further pulverized in a ball mill to obtain a particle size of <1 mm using standardized methods (ISO 18283 and ISO 13909-4). Because of the similarities in the qualitative XRF and qualitative XRD results for ashes derived from SA1 and SA2, with the exception of the inorganic elements and mineral contents (Collins, 2019), the SA2 sample was blended with 10% K_2CO_3 (7% K_2O) to prepare the SA2 blend. The K_2CO_3 was added during the ball milling step to ensure thorough mixing and to produce a homogeneous sample.

The SA2 blend ash sample was produced by thermal processing of the SA2 blend sample at 700°C. K_2O could increase the dissolution efficiency of K during alkaline leaching. Also, this potassium species in the SA2 blend ash may promote the formation of zeolite (sodalite) during NaOH leaching. The K_2CO_3 and NaOH, each of 99.5% purity, were provided by Ace Chemicals, South Africa. The NaOH was used to prepare 1 M (4%) and 8 M (32%) NaOH solutions for the leaching experiments. Proximate, ultimate, XRF, and XRD analyses were used to determine the chemical and mineralogical compositions of SA1 and SA2, as described in Collins (2019).

Ash samples

Each coal sample was split into four 5 kg sub-samples. The sub-samples were placed on fired clay trays and placed in the hot zone of a laboratory rotary kiln. The temperature of the kiln was increased to 700°C at a heating rate of 10°C/min. A residence time of 3 hours at 700°C was set for all the sub-samples. This step was conducted under an air flow rate of 80 ml/min to facilitate combustion of the organic components. Kaolinite, illite, muscovite, orthoclase, dolomite, calcite, pyrite, and added K_2CO_3 (in the SA2 blend) transformed at 700°C to form metakaolinite, heated K_2CO_3, and illite/orthoclase/muscovite amorphous materials. After 3 hours the laboratory rotary kiln was switched off and allowed to cool naturally to ambient temperature. The ash sub-samples were then removed from the kiln and blended to form one homogenous low-temperature combustion ash sample. These ash samples of SA1 and the SA2 blend were submitted for XRD and XRF analyses prior to the NaOH leaching experiments.

Production of sodium-based zeolites and a potassium-containing leach liqour by alkaline leaching
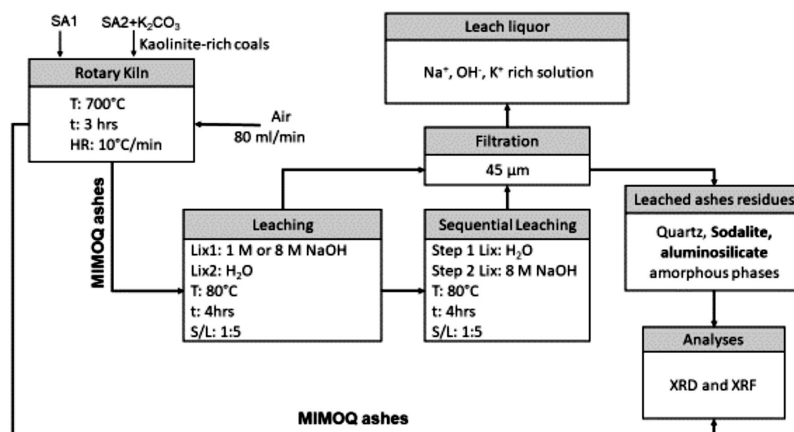

Figure 1—Schematic diagram of experimental procedures and analytical methods.
T: temperature, t: residence time, HR: Heating rate, S/L: solid to liquid ratio, Lix: lixiviant, MIMOQ ashes: metakaolinite and illite/muscovite/orthoclase/heated K_2CO_3 amorphous materials and quartz and K_2CO_3 containing SA1 and SA2 blend ashes

Analytical methods

XRF (Norrish and Hutton, 1969; ASTM D4326-13) and XRD analyses (Rietveld, 1969; Speukman, 2012) were employed to characterize the SA1 and SA2 blend ash samples and ashes produced from the H_2O and NaOH leaching procedures.

Experimental procedures

A schematic diagram showing the experimental procedure and analytical methods for coal and low-temperature combustion ash samples is presented in Figure 1.

Leaching experiments

H_2O leaching

Deionized water was used to dissolve Al, K, Si, and Ti containing compounds from the low-temperature combustion ash samples. Deionized water (100 ml) and 20 g of either SA1 ash or SA2 and K_2CO_3 blend ash were added to the leaching vessel for the water leaching experiments. The slurry was stirred at 200 r/min and a temperature of 80°C for 4 hours. The hot slurry was then filtered to produce a leached ash residue and leach liquor (filtrate). Sufficient deionized water (about 100 ml) was used to recover all dissolved species from the wet ash residue. The leach liquor was combined with the wash solution to produce the final leach liquor sample. The washed ash residue samples were dried at 60°C in a vacuum furnace and prepared to produce homogeneous solid samples for XRD and XRF analyses.

Alkaline leaching

The same leaching conditions and procedure that were used for the deionized water leaches were utilized in the alkaline leaching tests with either 1 M or 8 M NaOH as lixiviant. The washed and dried washed leached ash residues were submitted for XRD and XRF analyses.

Sequential leaching of ash with deionized water and 8 M NaOH

In the first sequential leaching procedure the washed ash residue from the deionized water leaches was returned to the leaching vessel and leached with 100 ml of 8 M NaOH solution using the deionized water leaching conditions to produce the final wet ash residue. The dried leached ash residue was prepared to yield homogeneous leached ash residue samples for XRD and XRF analyses.

For the second sequential leaching tests, the ash samples that were leached with 1 M NaOH were leached again with 8 M NaOH using the same conditions as for the deionized water leaching procedure. The final leached ash samples were washed with water to recover the dissolved inorganic species. Following the water washing step, the washed leached ash residues were dried and prepared to produce representative leached residue ash samples for XRD and XRF analyses.

Dissolution efficiencies of inorganic elements

The dissolution efficiencies of Al, K, Si and Ti into deionized water and alkaline solution were calculated using the XRF results for the original ash samples and the corresponding water-washed leached ash samples using Equation [1].

$$\eta(MO) = \frac{m\,(MO)_{CA} - m\,(MO)_{RES}}{m\,(MO)_{CA}} \times 100\% \qquad [1]$$

Where:
$\eta(MO)$ is the dissolution efficiency for the specific inorganic element (Al, K, Si and Ti);
$m(MO)_{CA}$ and $m(MO)_{RES}$ are the masses of inorganic elements in the coal ash and leached coal ash residue respectively (Jiang *et al.*, 2015).

Results and discussion

Coal composition, XRD and XRF analyses

Proximate and ultimate analyses of the SA1 and SA2 blend samples, together with XRD results for these coals, are presented and discussed in Collins (2019).

XRF and XRD analyses of coal ashes

XRF and XRD results for the SA1 and SA2 blend ash samples are presented in Table I. XRF analysis indicates that the SA1 ash contains high proportions of SiO_2 and Al_2O_3, with lesser proportions of the other oxides. The XRD results show that this material consists mainly of quartz and amorphous phases with smaller percentages (<2%) of other crystalline phases (Table I). The amorphous material consists primarily of metakaolinite (a transformed product of kaolinite), and lower proportions of illite/ muscovite/orthoclase amorphous phases. This is supported by the XRF and XRD results obtained by Bunt *et al.* (1998), where

Production of sodium-based zeolites and a potassium-containing leach liqour by alkaline leaching

Table I

Chemical and mineralogical compositions for the coal ash samples prepared at 700°C (wt. %)

Sample	SA1	SA2 blend	Sample	SA1	SA2 blend
SiO_2	61.9	36.5	Quartz	43.5	3.8
Al_2O_3	28.6	22.7	Calcite	-	8.0
K_2O	0.7	18.3	Anhydrite	1.5	1.2
CaO	2.9	8.8	Pseudomullite	1.4	-
Fe_2O_3	2.6	4.0	Hematite	1.4	1.2
TiO_2	2.0	1.8	Anorthite/orthoclase	1.1	0.8
SO_3	0.2	4.3	Portlandite	0.3	0.1
MgO	0.8	2.3	Magnetite	0.1	-
BaO	-	0.4	Magnetite	0.4	0.4
SrO	0.0	0.3	Cristobalite	0.1	0.1
ZrO_2	-	-	Gypsum	-	0.5
Cr_2O_3	0.1	0.1	Graphite	-	1.8
Na_2O	0.0	0.1	Diopside	-	4.4
P_2O_5	0.1	0.3	K_2CO_3	-	0.9
			Maghemite	0.2	-
			Pyrrhotite	0.5	0.4
			Kaolinite	-	0.6
			Amorphous	**49.5**	**75.8**

Table II

Chemical and mineralogical compositions of deionised water-leached ash (wt. %)

Sample	SA1	SA2 blend	Sample	SA1	SA2 blend
Lixiviant	**H_2O**	**H_2O**	**Lixiviant**	**H_2O**	**H_2O**
SiO_2	58.7	39.1	Quartz	35.6	3.0
Al_2O_3	27.	23.8	Calcite	1.1	8.8
K_2O	0.7	13.3	Illite	0.4	6.6
CaO	2.7	12.3	Hematite	1.7	4.1
Fe_2O_3	4.5	5.6	Anorthite/ortho	1.2	2.3
TiO_2	1.6	1.8	Clase/albeite		
SO_3	2.7	1.7	Anhydrite	0.1	0.7
MgO	1.1	1.2	Sodalite	-	0.5
BaO	0.5	0.6	Magnetite	0.4	0.4
SrO	0.0	0.3	Anatase	0.8	0.3
ZrO_2	0.1	0.1	Pseudomullite	-	0.3
Cr_2O_3	0.2	0.0	Portlandite	0.3	0.3
Na_2O	0.0	0.0	Gypsum	0.4	-
			Muscovite	0.5	-
			Maghemite	0.2	-
			Amorphous	**57.3**	**72.2**

the ash produced after subjecting coal fines to thermal processing in a rotary kiln at 600°C consisted of metakaolinite and other crystalline phases. The XRF results for the SA2 blend ash sample show that this sample is composed of higher proportions of SiO_2, Al_2O_3, K_2O, and CaO with minor proportions of SO_3, Fe_2O_3, TiO_2, MgO, P_2O_5, BaO, Na_2O, and SrO. The higher K percentage (18% K_2O compared to 1% K_2O (Collins, 2019)) in the SA2 blend ash is due to the addition of K_2CO_3 to the SA2 coal. The SA2 blend ash sample has a higher amorphous content with smaller percentages of quartz and anorthite than the SA1 ash sample. Calcium oxide can react with metakaolinite at elevated temperatures to form anorthite (Hlatshwayo *et al.*, 2009; Rautenbach *et al.*, 2020). Diopside is formed from reactive silica reacting with high-temperature carbonate products (CaO or mixture of CaO and MgO (Hlatshwayo *et al.*, 2009; Matjie *et al.*, 2008).
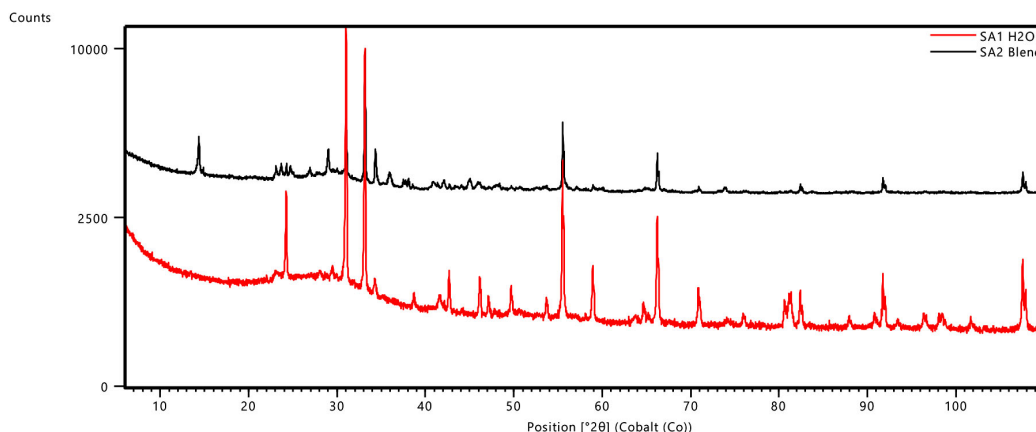
Figure 2—Diffractograms of SA1 and SA2 blend ash samples leached with deionized water

H₂O leaching

XRF and XRD results for the water-leached ash samples are presented in Table II and Figure 2 respectively. It is clear from a comparison of Tables I and II that the water-leached ash samples yielded similar qualitative XRF, but different qualitative XRD, results compared to those of the original ash samples before leaching, with the exception of chemical and mineralogical compositions. The proportion of K_2O in the SA2 blend ash sample decreased during water leaching. This can be attributed to the dissolution of the added K_2CO_3 in water:

$$K_2CO_3 + 2H_2O \rightarrow 2KOH + H_2O + CO_2 \qquad [2]$$
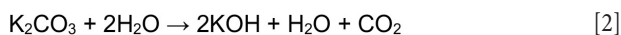
This could imply that almost all the inorganic compounds in the SA1 and SA2 blend ash samples are insoluble in water. The crystalline mineral contents of the leached ash samples decreased slightly compared to the original ash samples due to the slight increase in the amorphous and sodalite contents in the water-leached SA2 blend ash samples (Tables I and II; Figure 2). Available Na_2O from the ash samples could react with water, and the subsequently formed KOH can react with metakaolinite to form a small proportion of sodalite in the water-leached SA2 blend ash sample. The potassium hydroxide may promote the formation of zeolite (Murayama, Yamamoto, and Shibata, 2002).

Alkaline leaching

XRF analysis

XRF results for the ash samples leached with 1 M NaOH and 8 M NaOH are presented in Table III. Leaching of SA1 ash with 1 M NaOH resulted in a slight decrease in the SiO_2 and Al_2O_3 concentrations, possibly due to the dissolution of metakaolinite and quartz in the sodium hydroxide lixiviant. The solubility of silica in NaOH is well known (Rattanasak and Chindaprasirt, 2009) (Equation [3]). After leaching of the SA1 ash samples with either 1 M or 8 M NaOH, the XRF analysis shows a decrease in SiO_2 and Al_2O_3 concentrations, as expected, compared to the original ash samples and water-leached ashes (Tables I and III). The increase in the CaO concentration in the SA2 blend ash sample leached with 8 M NaOH may be due to the dissolution of K_2O and insolubility of CaO in this lixiviant. Also, leaching of the SA2 blend ash with 8 M NaOH dissolved a significant amount of K_2O, with the K_2O concentration decreasing from 18.3% (Table

I) to 5.1% (Table III). The XRF results for SA1 and SA2 blend leached with 1 M NaOH show only minor changes in the elemental compositions compared to those of the original ash samples (Tables I and III).

XRD analysis

XRD results for the ash samples leached with 1 M and 8 M NaOH are presented in Table IV and Figures 3 and 4. The results indicate a decrease in the quartz content, which can be attributed to the dissolution of quartz in the sodium hydroxide solution (Rahman, Pudasainee, and Gupta, 2017; Su *et al.*,(2011):

$$SiO_2 + 2NaOH \rightarrow Na_2SiO_3 + H_2O \text{ or } (Na_2SiO_2(OH)_2) \qquad [3]$$
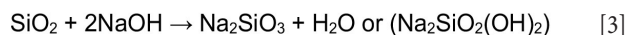
This decrease is partially due to dissolution of the metakaolinite and quartz in sodium hydroxide solution to form an amorphous precipitate (sodalite gel precursor) $(Na_8Al_6Si_6O_{24}. (OH)_2.2H_2O)$ and sodalite, which subsequently crystallizes from this amorphous material (Equation [4]). The sodium hydroxide leached ash samples contained 11% to 18% sodalite (Tables II, IV and VI; Figures 2-6, 9).

The possible reaction of hydrated metakaolinite or kaolinite and sodium hydroxide to form sodalite during the NaOH leaching is as follows (Rahman, Pudasainee, and Gupta, 2017; Yang, Zheng, and Zhang, 2014; Su *et al.*, 2011).

$$3Al_2Si_2O_5(OH)_4 + 8NaOH \rightarrow Na_8Si_6Al_6O_{24}(OH)_2 + 9H_2O \qquad [4]$$

The increase in the amorphous material could be attributed to the formation of sodium alumino-silicate gel in the leached ash samples and subsequent crystallization of sodalite from this phase. XRD analysis of the ash samples shows a slight decrease in calcite concentration from 8.3% to 5.3% as the concentration of Ca/K/Na–feldspars increases from 0.8% to 7.4%. Other changes observed in the mineral composition include a decrease in diopside concentration from 4.4% to zero and an increase in illite from zero to 4.6%. Matjie *et al.* (2021), Rautenbach *et al.* (2020) and Rautenbach *et al.* (2021) state that $Al_2O_3 \cdot 2SiO_2$ reacts with K^+ from the added potassium species to form K-feldspar in the chars and coal ashes upon pyrolysis and combustion of South African feed-coals. A lower pseudomullite proportion was also noted in the SA2 blend ash sample. These minerals present in the leached SA2 blend ash residue are insoluble in alkaline solution. The amorphous material and quartz concentrations show only minor changes compared to the original SA2 blend ash (Tables I and IV).

Production of sodium-based zeolites and a potassium-containing leach liqour by alkaline leaching

The increased sodium concentration was supported by the presence of sodalite (11%) in the leached ash residues (Table IV, Equation [4]). The calcite concentration decreased from 8% to 0.3% as the Ca/K/Na–feldspars concentration increased from 1.7% to 6%. Mineralogical changes were seen in the XRD results due to the dissolution of alkaline-soluble compounds and formation of sodalite and amorphous materials in the ash leached with sodium hydroxide solution.

Minimal changes to the mineralogical composition of the leached ash residue samples were noted (Tables I and II). Leaching of the SA1 and SA2 blend ash samples with 8 M NaOH not only removed alkaline-soluble compounds, but also transformed the metakaolinite in the ash samples to sodalite (Hassan and Crundy,1983).

Sequential leaching

XRF and XRD analyses

XRF results for the leached ash samples produced by the two sequential leaching procedures are presented in Table V. XRF analysis of the leached SA1 ash residue indicates that the concentrations of SiO_2, Al_2O_3, and K_2O decreased during leaching with H_2O and 8 M NaOH, while the proportion of Na_2O increased,

as expected. This implies that metakaolinite and quartz dissolved in the sodium hydroxide solution. XRF analysis of the water-leached SA1 ash residue and the SA1 ash shows that SiO_2 and Al_2O_3 in the SA1 ash decreased during H_2O and 8 M NaOH leaching. As expected, the proportion of Na_2O increased in the leached SA1 ash residue after H_2O and NaOH leaching. This implies that Al_2O_3 and SiO_2, which are associated with metakaolinite in the SA1 ash, were dissolved in the sodium hydroxide solution to form sodalite precipitate gel, significantly reducing the quartz content and increasing the total amorphous content (Table VI, Figures 5 and 6). XRD analysis detected sodalite, calcite, and Ca/K/Na–feldspars in the leached SA1 ash residue (Figures 5 and 6). These minerals do not occur in the original SA1 ash sample (Tables I and VI).

Table III

Chemical composition for the coal ash residues after leaching with 1 M and 8 M NaOH solutions (wt. %)

Sample	SA1		SA2 blend	
NaOH Concentration	1 M	8 M	1 M	8 M
SiO_2	58.3	50.5	37.8	34.2
Al_2O_3	25.9	23.1	23.5	21.6
Na_2O	2.4	14.7	1.6	15.7
CaO	3.0	2.8	12.8	11.0
K_2O	0.7	0.3	12.6	5.1
Fe_2O_3	4.8	4.1	4.8	4.9
SO_3	1.1	1.1	1.6	2.6
MgO	1.2	1.0	2.4	2.0
TiO_2	1.6	1.5	1.9	1.8
BaO	0.5	0.6	0.5	0.6
SrO	0.0	0.0	0.3	0.3
ZrO_2	0.1	0.1	0.1	0.0
Cr_2O_3	0.1	0.1	0.0	0.0

Table IV

Mineralogical composition for the coal ash residue after leaching with 1 M and 8 M NaOH solutions

Sample	SA1		SA2 blend	
NaOH Conc.	1 M	8 M	1 M	8 M
Ca/K/Na–feldspars	1.7	1.6	7.4	6.0
Quartz	30.3	21.6	2.7	1.8
Sodalite	-	16.5	-	11.4
Calcite	1	0.4	5.3	0.3
Illite	-	-	4.6	-
Pseudomullite	-	-	1.5	0.2
Magnetite	0.3	0.5	0.4	0.3
Portlandite	-	-	0.1	3.9
Haematite	1.4	0.7	-	-
Anatase	0.4	0.4	-	-
Graphite	0.1	-	-	-
Periclase	0.2	0.3	0.5	-
Cristobalite	0.1	-	-	-
Diopside	0.1	-	-	-
Dolomite	0.3	-	-	-
Gypsum	0.3	0.4	-	0.5
Maghemite	0.2	0.3	-	-
Muscovite	0.1	-	-	0.6
Rutile	-	-	-	1.3
Amorphous phases	**63.6**	**57.1**	**77.4**	**73.7**

Note: Conc. = Concentration
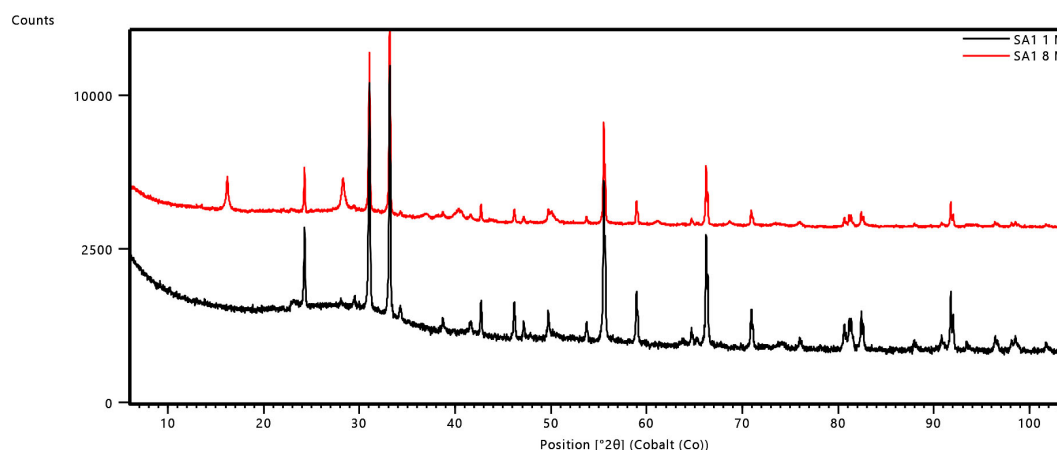
Figure 3–Diffractograms of SA1 ash leached with 1 M and 8 M NaOH
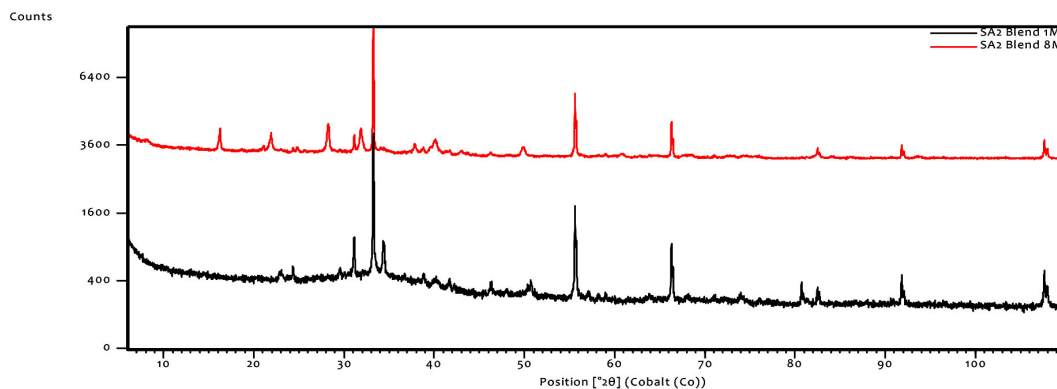
Figure 4–Diffractograms of SA2 blend ash leached with 1 M and 8 M NaOH

XRF results for the SA2 blend ash sample show a significant decrease in the K_2O concentration, from 18% to 2% (Table V), after leaching with either H_2O and 8 M NaOH, or 1 M NaOH and 8 M NaOH solutions. This can be ascribed to the high solubility of potassium species in water and sodium hydroxide solution (Equation [5]). The SiO_2 and Al_2O_3 contents decreased and the Na_2O content increased from 0.1% to 15.3% during the sequential H_2O/I M NaOH and 8 M NaOH leaching tests (Tables I and V). The higher proportion of Na_2O in the leached SA2 blend ash residue is due to the formation of zeolite phases in this sample (Equation [4]).

Finally, the reaction between potassium carbonate and sodium hydroxide to form sodium carbonate and potassium hydroxide in the leach liquors can catalyze the reaction of sodalite during NaOH leaching of the SA2 blend ash (Murayama, Yamamoto, and Shibata, 2002; Equation [4]). The possible chemical reaction between potassium carbonate and sodium hydroxide is as follows:

$$K_2CO_3 + 2NaOH \rightarrow Na_2CO_3 + 2KOH \qquad [5]$$
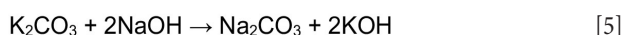
On cooling this amorphous material to room temperature, sodalite crystallized (Equation [4]; Figures 5 and 6). The final ash residues produced after the sequential leaching of the original ash are characterized by high proportions of sodalite, Na_2O, and amorphous materials, and low proportions of quartz and K_2O compared to those of the original ash samples (Tables I – VI).

Table V

Chemical composition of the ash residues after sequential leaching (H_2O and 8 M NaOH and 1 M and 8 M NaOH solutions) (wt. %)

Sample	SA1		SA2 blend	
Lixiviant Step1/ Step 2	H_2O/8 M	1M/8M	H_2O/8M	1 M/8 M
SiO_2	50.1	50.5	35.8	35.1
Al_2O_3	22.6	21.9	22.5	21.6
Na_2O	15.8	15.1	15.3	14.7
CaO	2.3	2.8	12.5	14.4
Fe_2O_3	4.0	4.5	5.7	5.6
MgO	0.8	1.1	1.9	2.4
K_2O	0.3	0.3	2.2	2.0
TiO_2	1.4	1.5	2.0	1.9
SO_3	1.9	1.3	1.4	1.1
BaO	0.5	0.5	0.3	0.6
SrO	0.0	0.0	0.3	0.3
ZrO_2	0.1	0.1	0.0	0.1
Cr_2O_3	0.1	0.1	0.0	0.0

Table VI

Mineralogical composition for the ash residues after sequential leaching (H_2O and 8 M NaOH and 1 M and 8 M NaOH solutions) (wt. %)

| Sample	SA1		SA2 blend	
Lixiviant Step1/ Step 2	H_2O/8 M	1 M/8 M	H_2O/8 M	1 M/8 M
Sodalite	17.6	15.5	16.9	17.9
Quartz	18.6	17.3	2.8	2.8
Illite	-	-	3.3	1.2
Haematite	0.7	0.6	2.6	2.0
Ca/K/Na–feldspars	2.9	4.0	2.4	0.1
Portlandite	-	-	1.0	0.5
Calcite	0.3	0.3	0.7	0.8
Pseudomullite	-	-	0.5	0.4
Magnetite	0.3	0.1	0.3	0.3
Anatase	0.2	0.2	0.2	0.1
Periclase	0.1	0.1	0.1	-
Maghemite	0.3	0.2	0.1	0.2
Rutile	-	-	0.1	0.1
Fluorapatite	0.3	0.4	-	-
Graphite	-	-	-	0.2
Cristobalite	0.1	0.1	-	-
Diopside	-	-	-	0.2
Dolomite	-	0.1	-	-
Muscovite	-	-	-	0.6
Amorphous	**58.6**	**61.0**	**68.7**	**72.1**
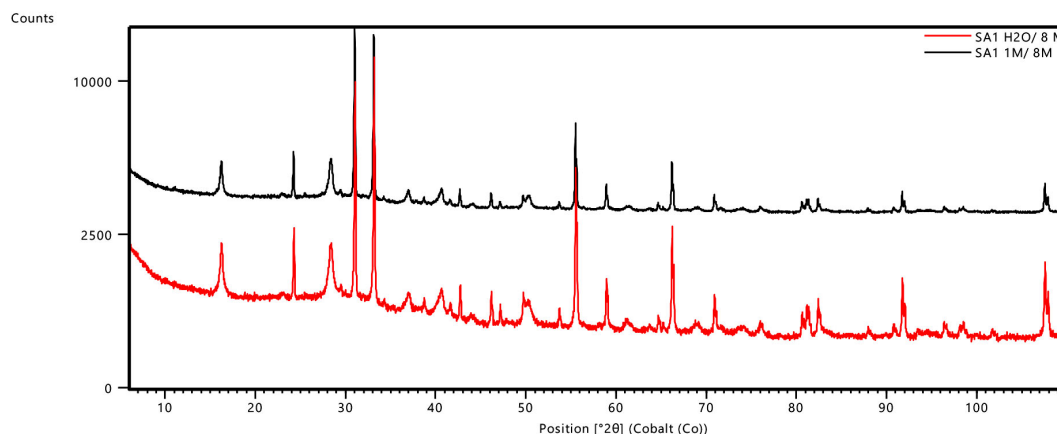
Figure 5—Diffractograms of sodalite-containing SA1 ash leached with water followed by 8 M NaOH, and with 1M NaOH followed by 8M NaOH
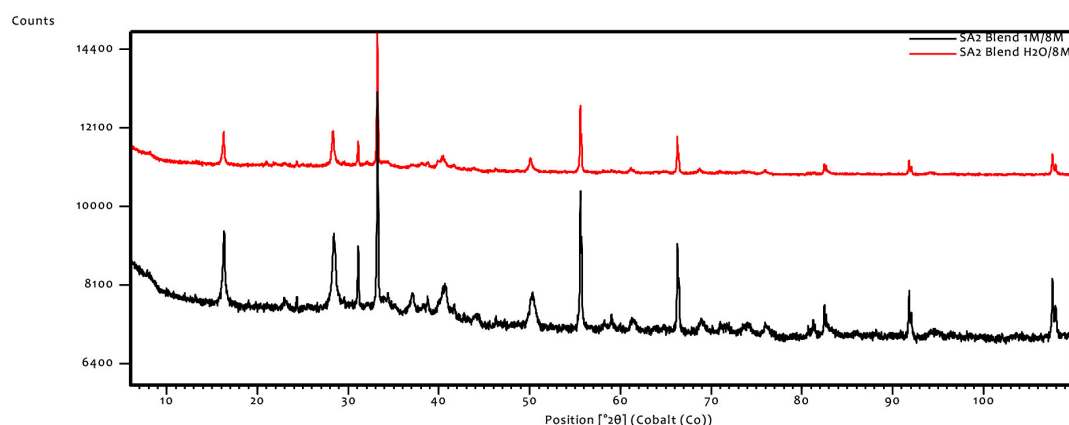

Figure 6—Diffractograms of sodalite-containing SA2 blend ash leached with water followed by 8 M NaOH, and with 1 M NaOH followed by 8 M NaOH

Dissolution efficiencies of inorganic elements (Al, K and Ti)

The dissolution efficiencies for Al, K, and Ti, calculated from the XRF results for the SA1 and SA2 blend ash samples and the corresponding leached ash residues, are presented in Figure 7. Water leaching resulted in low dissolution efficiencies of Al, K, and Ti. The highest K dissolution efficiency (33.4%) for the SA2 blend ash is due to the dissolution of K_2CO_3 in water (Equation [1]).

Leaching of the SA1 ash sample in 1 M NaOH yielded low dissolution efficiencies of Al, K, and Ti. With 8 M NaOH leaching the dissolution efficiency of K increased to 57.6%, while the values for Al and Ti were relatively unchanged. This was as expected, owing to to the reaction between NaOH and K_2CO_3. Leaching the SA2 blend ash sample with 1 M NaOH yielded only low dissolution efficiencies of Al, K, and Ti. With 8 M NaOH leaching the dissolutions of Al and Ti were zero or negative, and for K the highest dissolution efficiency (70.5%). The negative or low calculated dissolution values indicate that the dissolved Al and Si in the lixiviants co-precipitated with Na^+ ions into the leached ash to form sodalite gel precursor (Tables IV and VI, Figure 7). Sodalite subsequently crystallized at lower temperatures from this amorphous precipitate. Both sodalite and amorphous phases (Na-K-Ti-Ca-aluminosilicates) in the leached ash residues are accountable for the negative or low dissolution efficiencies of inorganic elements.

The sequential leaching tests of the SA1 ash sample with either H_2O or 1 M NaOH followed by 8 M NaOH achieved low dissolution efficiencies of Al and Ti, and a high K dissolution efficiency (57–60%). This suggests either that the lixiviant concentrations were too low for dissolution of soluble minerals and metakaolinite, or that dissolved metakaolinite/quartz ions precipitated with Na^+ ions to form sodalite. Sequential leaching of the SA2 blend ash sample with H_2O followed by 8 M NaOH yielded dissolution efficiencies of 0% Al, 88% K, and 0% Ti; and 8.7% Al, 89.6% K, and 0% Ti when leaching with 1 M NaOH followed by 8 M NaOH. The high potassium dissolution efficiency values can be ascribed to the solubility of the potassium species from the heated SA2 blend ash during NaOH leaching (Equation [5]). Some potassium ions did not react with metakaolinite or crystallize together with the sodalite after leaching with sodium hydroxide solutions. Other K^+ ions could have reacted with OH^- ions from the sodium hydroxide solution to form potassium hydroxide (Equation [5]). Other Na^+ ions could react with CO_3^{2-} ions from K_2CO_3 to form sodium carbonate. This reaction between potassium carbonate and sodium hydroxide may adversely affect sodalite formation. The low dissolution efficiency values of Al and Si during sequential leaching are associated with sodalite and aluminosilicate formation. Sakthivel et al. (2013) heated a mixture of alkali compound and CFA to form zeolite in the ash. Fukasawa et al. (2017) thermally treated a mixture of CFA and NaOH in a microwave oven at 85°C to form aluminosilicate-gel precipitate from which hydrosodalite crystallized. Jiang et al. (2015) heated a blend of fly ash derived from the incineration of municipal
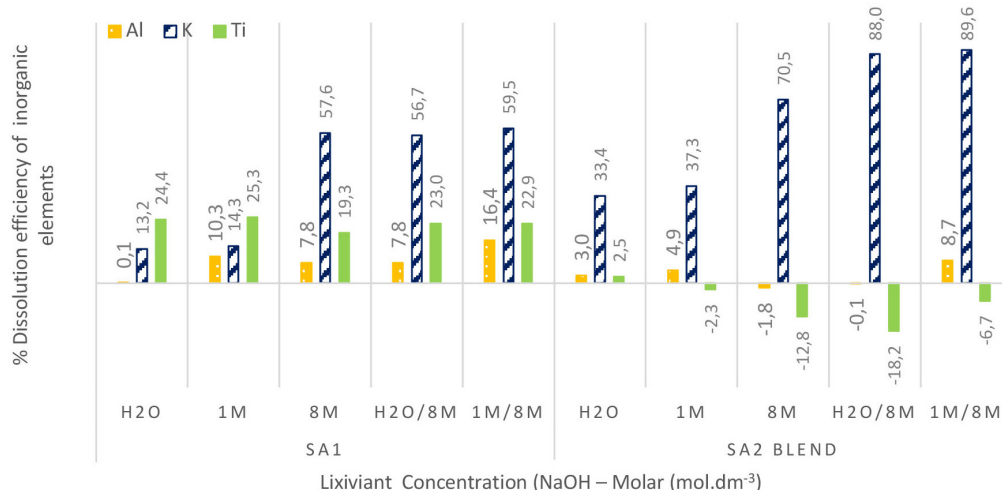
Figure 7—Dissolution efficiencies for Al, K, and Ti as calculated from XRF results of ash and leached ash residue samples. Note: Sodalite and alumino-silicate formations in the leached ash residues is associated with either low or negative dissolution efficiency values of inorganic elements
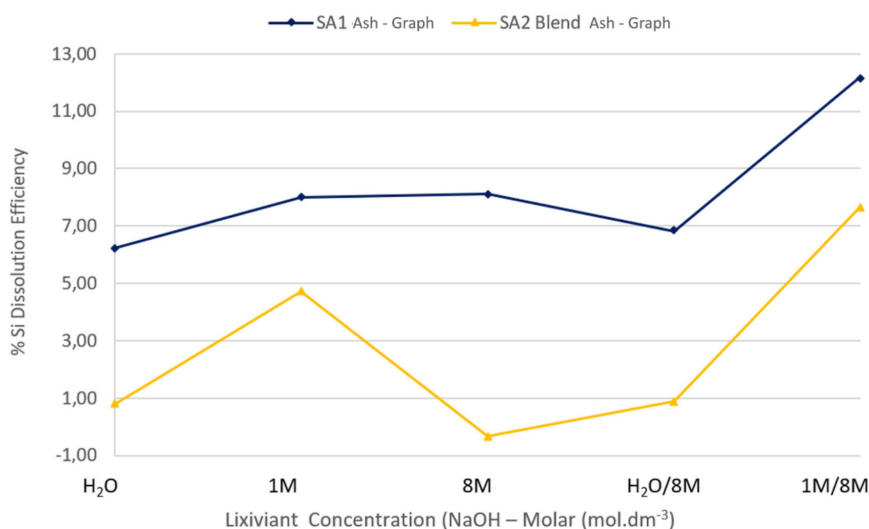

Figure 8– Dissolution efficiencies for Si as calculated from the XRF results for the original ashes and corresponding leached ashes

solid waste and Na_2HPO_4 at 200°C for 30 minutes to produce zeolite in the ash. All zeolite formation in the ash or solid samples resulted in the negative, low or zero dissolution efficiencies for Al and Si from the coal ash sample during alkaline leaching (Figures 7 and 8).

Dissolution efficiency of Si

The dissolution efficiency values of Si are depicted in Figure 8. Leaching of the SA1 and SA2 blend ash samples with H_2O showed low dissolution efficiencies for Si due to the negligible solubility of Si in water. Low Si dissolution efficiencies were also achieved in 1 M and 8 M NaOH. This can be attributed to the precipitation of either dissolved metakaolinite (SiO_3^{2-}, $Al(OH)_4^-$), or quartz, and Na^+ to form sodalite gel precursor in the leached ash residues. The low Si dissolution efficiency values resulted due to precipitation of these ions from the sodium hydroxide leach liquors and are consistent with results reported by Su *et al.* (2011); Fukasawa *et al.* (2017); Jiang *et al.* (2015); Rahman, Pudasainee, and Gupta (2017), and Yang, Zheng, and Zhang (2014).

Sodium oxide and sodalite percentages in the original and leached ash samples

The percentages of sodium oxide (XRF results) and sodalite (XRD results) in the original ash and ash residue samples are depicted in Figure 9. The SA1 and SA2 blend ash samples, before water leaching, contained no sodium or sodalite (zeolite phase); this phase only appeared after leaching with H_2O. As expected, a small increase in the sodium concentration was seen after leaching the SA1 and SA2 blend ash samples with 1 M NaOH. Leaching of the SA1 ash sample with 8 M NaOH solution led to the formation of 14.7% of Na_2O and 16.5% sodalite in the ash residue. This same trend was seen after NaOH leaching of the SA2 blend ash sample, which resulted in a 15.7% Na_2O and 11% sodalite content in the residues. Murayama, Yamamoto, and Shibata (2002) found that zeolite crystallization decreases in the presence of high potassium (K^+) concentrations. Based on the XRD results for the leached SA1 and SA2 blend ash residues in Table IV, the addition of K_2CO_3 to

Production of sodium-based zeolites and a potassium-containing leach liqour by alkaline leaching
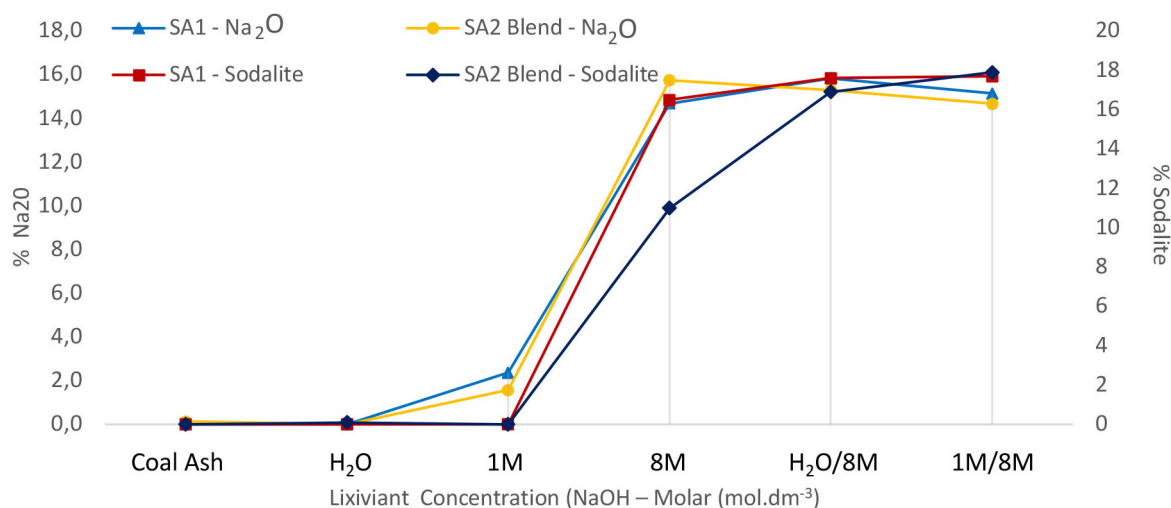

Figure 9—Na₂O in ash/ash residue (by XRF, %) versus lixiviant concentration – molar (M) versus sodalite in ash/ash residue by XRD, %)

the SA2 sample inhibited sodalite crystallization. Other sodium ions can react with carbonate ions from potassium carbonate to form sodium carbonate in the leach liquor. This reaction may subsequently reduce the formation of a high proportion of sodalite in the ash residues during sodium hydroxide leaching (Equation [5]).

As expected, the residues from sequential water leaching (zero Na₂O) or 1 M NaOH leaching (a low proportion of Na₂O) of the SA1 ash samples contained lower proportions of sodium oxide and sodalite compared to the samples leached with 1 M NaOH and 8 M NaOH. Sequential leaching of the SA2 blend ash sample with 8 M NaOH leads to an increase in sodalite concentration (>15%) in the ash residue. Murayama, Yamamoto, and Shibata (2002) stated that OH⁻ from either KOH or NaOH promotes the reactions for zeolite formation (Equations [2 and 4]). Jiang *et al.* (2015) explained that, after the initial dissolution of aluminosilicate and zeolite crystal, equilibrium is reached between the zeolite and soluble SiO_3^{2-} and $Al(OH)_4^-$ anions. Changing the leaching conditions will disrupt the equilibrium and formation of zeolite will again be initiated.

Conclusions

South African low-temperature combustion ash produced at 700°C was leached in alkaline media in an attempt to solubilize SiO_3^{2-} and $Al(OH)_4^-$ ions from metakaolinite in the ash and form synthetic sodium zeolite for possible use in the water purification industries or as molecule separators. The recovery of potassium species for utilization in the fertilizer industry was also investigated. The leaching of the SA1 ash sample with H₂O and 1 M and 8 M NaOH solutions yielded only low dissolution efficiencies of Si, Al, Ti, and K compared to the SA2 blend samples (with added K₂CO₃) leached with 1 M and 8 M NaOH. A high dissolution efficiency of 89% K was achieved by sequential leaching of the SA2 blend ashes using 1 M and 8 NaOH. Small percentages of Al and Si dissolution resulted due to the formation of sodalite precursor gel in the leached ashes after sequential leaching with 1 M and 8 M NaOH. Crystallization of sodalite from the sodalite precursor gel

(amorphous material) resulted in the formation of aluminosilicate glasses. The increase in NaOH concentration from 1 M to 8 M NaOH resulted in a higher proportion of sodalite (16.5%) forming in the SA1 ash residue. A lower proportion of sodalite (11%) was formed in the SA2 blend ash residue due to the reaction between potassium carbonate and sodium hydroxide.

The formation of higher proportions of sodalite and amorphous materials in the leached ash residues resulted in different mineralogical and chemical properties of ash residues during the sequential NaOH leaching of the SA1 and SA2 blend ashes.

To improve the proportion of sodalite in the leached ash, the mixture of the spent potassium carbonate (waste) from the thermo-chemical plants and coal fine discards (waste), as well as coal fines, could be combusted at 700°C to produce potassium- and metakaolinite-containing ash and low-temperature combustion ash for the proposed alkaline leaching process using 12-20 M NaOH. Furthermore, ash-derived zeolites, as well as the low-temperature combustion ashes, should be submitted for morphological characterization, XRD, and particle size distribution analyses using high-resolution transmission electron microscopy (HRTEM) or scanning electron microscopyusing energy dispersive X-ray spectroscopy (SEM-EDS) and Raman techniques.

Production of sodium-based zeolites and a potassium-containing leach liqour by alkaline leaching

References

ADRIAN, A. and MCCULLOCH, H. 1966. Pressure leaching of ores with particular reference to the upgrading of aluminate solutions. II. Alkaline pressure leaching of Sasol fly ash. Government Metallurgical Laboratory. (Repub. SA), no. C 13/65. 13 pp.

BUKHARI, S.S., BEHIN, J., KAZEMIAN, H., and ROHANI, S. 2015. Conversion of coal fly ash to zeolite utilizing microwave and ultrasound energies: a review. *Fuel*, vol. 140. pp. 250–266.

BUNT, J.R., VAN NIEROP, P., MATJIE, R.H., RITTER, B., STEYNBERG, E.C., and KATABUA, M.J. 1998. South Africa patent no. 98/583.

BUNT, J.R., NEOMAGUS, H.W.J.P., BOTHA, A.A., and WAANDERS, F.B. 2015. Reactivity study of fine discard coal agglomerates. *Journal of Analytical and Applied Pyrolysis*, vol. 113. pp. 723–728. https://doi.org/10.1016/j.jaap.2015.03.001

COLLINS, A.C. 2019. Extraction of K, AI and Ti containing compounds from ash produced by low temperature combustion. PhD thesis, North-West University. Chapter 4, Section 4.2.2.

COMRIE, D.C. and KRIVEN, W.M. 2004. Composite cold ceramic geopolymer in a refractory application. *Proceedings of Advances in Ceramic Matrix Composites IX*, Nashville, TN. Wiley. pp. 211–225.

FUKASAWA, T., KARISMA, A.D., SHIBATA, D., HUANG, A.-N., and FUKUI, K. 2017. Synthesis of zeolite from coal fly ash by microwave hydrothermal treatment with pulverization process. *Advanced Powder Technology*, vol. 28, no. 3. pp. 798–804.

HASSAN, I. and CRUNDY, H.D. 1983. Structure of basic sodalite, $Na_8Al_6Si_6O_{24}$ $(OH)_2$. $2H_2O$. *Acta Crystallographica*, vol. C39. pp. 3–5.

HLATSHWAYO, T.B., MATJIE, R.H., LI, Z., and WARD, C.R. 2009. Mineralogical characterisation of Sasol feed coals and corresponding gasification ash constituents. *Energy and Fuels*, vol. 23. pp. 2867–2873.

IZQUIERDO, M. and QUEROL, X. 2012. Leaching behaviour of elements from coal combustion fly ash: An overview. *International Journal of Coal Geology*, vol. 94. pp. 54–66.

JIANG, Z., YANG, J., MA, H., WANG, L., and MA, X. 2015. Reaction behaviour of Al_2O_3 and SiO_2 in high alumina coal fly ash during alkali hydrothermal process. *Transactions of Nonferrous Metals Society of China*, vol. 25. pp. 2065–2072.

KING, J.F., TAGGART, R.K., SMITH, R.C., HOWER, J.C., and HSU-KIM, H. 2018. Aqueous acid and alkaline extraction of rare earth elements from coal combustion ash. *International Journal of Coal Geology*, vol. 195. pp. 75–83.

LI, H., JUNBO, H., WANG, C., BAO, W., and SUN, Z. 2014. Extraction of alumina from coal fly ash by mixed-alkaline hydrothermal method. *Hydrometallurgy*, vol. 147-148. pp. 183–187.

MATJIE, R.H., LI, Z., WARD, C.R., and FRENCH, D. 2008. Chemical composition of glass and crystalline phases in coarse coal gasification ash. *Fuel*, vol. 87. pp. 857–869.

MATJIE, R.H., LI, Z., WARD, C.R., KOSASI, J., BUNT, J.R., and STRYDOM, C.A. 2015. Mineralogy of furnace deposits produced by South African coals during pulverized-fuel combustion tests. *Energy and Fuels*, vol. 29. pp. 8226–8238.

MATJIE, R., BUNT, J., STOKES, W., BIJZET, H., MPHAHLELE, K., UWAOMA, R., and STRYDOM, C. 2021. Interactions between kaolinite, organic matter, and potassium compounds at elevated temperatures during pyrolysis of caking coal and its density-separated fractions. 2021. *Energy and Fuels*, vol. 35. pp. 13268–13280.

MURAYAMA, N., YAMAMOTO, H., and SHIBATA, J. 2002. Mechanism of zeolite synthesis from coal fly ash by alkali hydrothermal reaction. *International Journal of Mineral Processing*, vol. 64, no. 1. pp. 1–17.

NAYAK, N. and PANDA, C.R. 2010. Aluminium extraction and leaching characteristics of Talcher Thermal Power Station fly ash with sulphuric acid. *Fuel*, vol. 89. pp. 53–58.

NORRISH, K., and HUTTON, J.T. 1969. An accurate X-ray spectrographic method for the analysis of a wide range of geological samples. *Geochimica et Cosmochimica Acta*, vol. 33, no. 4. pp. 431–453.

RAHMAN, M., PUDASAINEE, D., and GUPTA, R. 2017. Review on chemical upgrading of coal: Production processes, potential applications and recent developments. *Fuel Processing Technology*, vol. 158. pp. 35–56.

RATTANASAK, U. and CHINDAPRASIRT, P. 2009. Influence of NaOH solution on the synthesis of fly ash geopolymer. *Minerals Engineering*, vol. 22, no. 12. pp. 1073–1078.

RAUTENBACH, R., STRYDOM, C.A., BUNT, J.R., MATJIE, R.H., CAMPBELL, Q.P., and VAN ALPHEN, C. 2019. Mineralogical, chemical, and petrographic properties of selected South African power stations' feed coals and their corresponding density separated fractions using float-sink and reflux classification methods. *International Journal of Coal Preparation and Utilization*, vol. 39. pp. 421–446.

RAUTENBACH, R., MATJIE, R.H., STRYDOM, C.A., and BUNT, J.R. 2021. Transformation of inherent and extraneous minerals in feed coals of commercial power stations and their density-separated fractions. *Energy Geoscience*, vol. 2. pp. 136–147. https://doi.org/10.1016/j.engeos.2020.09.002

RAUTENBACH, R., MATJIE, R.H., STRYDOM, C.A., BUNT, J.R., WARD, C.R., FRENCH, D., and VAN ALPHEN, C. 2020. Evaluation of mineral matter transformations in low-temperature ashes of South African coal feedstock samples and their density separated cuts using high-temperature X-ray diffraction. *International. Journal of Coal Preparation and Utilization*, vol. 40, no. 4-5. pp. 320–347. doi: 10.1080/19392699.2019.1677629

REDDICK, J.F., VON BLOTTNITZ, H., and KOTHUIS, B. 2007. A cleaner production assessment of the ultra-fine coal waste generated in South Africa. *Journal of the Southern African Institute of Mining and Metallurgy,* vol. 107. pp. 55–60.

RIETVELD, H.M. 1969. A profile refinement method for nuclear and magnetic structures. *Journal of Applied Crystallography*, vol. 2. pp. 65–71.

SAKTHIVEL, T., REID, D.L., GOLDSTEIN, I., HENCH, L., AND SEAL, S. 2013. Hydrophobic high surface area zeolites derived from fly ash for oil spill remediation. *Environmental Science and Technology*, vol. 47, no. 11. pp. 5843–5850.

SANGITA, S., NAYAK, N., and PANDA, C.R. 2017. Extraction of aluminium as aluminium sulphate from thermal power plant ashes. *Transactions of Nonferrous Metals Society of China*, vol. 27. pp. 2082–2089.

SPEAKMAN, S.A. 2012. Basics of X-ray powder diffraction. http://prism.mit.edu/xray [accessed 14 February 2019].

SU, S.Q., YANG, J., MA, H.W., JIANG, F., LIU, Y.Q., and LI, G. 2011. Preparation of ultrafine aluminum hydroxide from coal fly ash by alkali dissolution process. *Integrated Ferroelectrics*, vol. 128, no. 1. pp. 155–162.

VAN ALPHEN, C. 2005. Factors influencing fly ash formation and slag deposit formation (slagging) on combusting a South African pulverised fuel in a 200MWe boiler. PhD thesis, University of the Witwatersrand.

VAN DER MERWE, E.M., GRAY, C.L., CASTLEMAN, B.A., MOHAMED, S., KRUGER, R.A., and DOUCET, F.J. 2017. Ammonium sulphate and/or ammonium bisulphate as extracting agents for the recovery of aluminium from ultrafine coal fly ash. *Hydrometallurgy*, vol. 171. pp. 185–190.

YANG, Q.-C., ZHENG, S.-I., and ZHANG, R. 2014. Recovery of alumina from circulating fluidized bed combustion Al-rich fly ash using mild hydrochemical process. *Transactions of Nonferrous Metals Society of China*, vol. 24, no. 4. pp.1187–1195. ◆